

# The connection between the gamma-ray emission and millimeter flares in Fermi/LAT blazars

J. León-Tavares, M. Tornikoski, A. Lähteenmäki  
*Aalto University Metsähovi Radio Observatory,  
 Metsähovintie 114, FIN-02540 Kylmälä, Finland.*

E. Valtaoja  
*Tuorla Observatory, Department of Physics and Astronomy, University of Turku, 20100 Turku, Finland.*

E. Nieppola  
*Finnish Centre for Astronomy with ESO (FINCA),  
 University of Turku, Väisäläntie 20, FI-Piikkiö, Finland.*

We compare the  $\gamma$ -ray photon flux variability of northern blazars in the *Fermi*/LAT First Source Catalog with 37 GHz radio flux density curves from the Metsähovi quasar monitoring program. We find that the relationship between simultaneous millimeter (mm) flux density and  $\gamma$ -ray photon flux is different for different types of blazars. The flux relation between the two bands is positively correlated for quasars and does not exist for BLLacs. Furthermore, we find that the levels of  $\gamma$ -ray emission in high states depend on the phase of the high frequency radio flare, with the brightest  $\gamma$ -ray events coinciding with the initial stages of a mm flare. The mean observed delay from the beginning of a mm flare to the peak of the  $\gamma$ -ray emission is about 70 days, which places the average location of the  $\gamma$ -ray production at or downstream of the radio core. We discuss alternative scenarios for the production of  $\gamma$ -rays at distances of parsecs along the length of the jet .

## I. INTRODUCTION

Several studies, based on the first year of Fermi/LAT operations, have shown that: (i) the  $\gamma$ -ray and the averaged radio flux densities are significantly correlated [e.g. 1] and (ii) blazars detected at  $\gamma$ -rays are more likely to have larger Doppler factors and larger apparent opening angles than those not detected by LAT [e.g. 2]. This observational evidence strongly suggests that radio and  $\gamma$ -ray emission have a co-spatial origin. To locate and identify the region where the bulk of  $\gamma$ -ray emission is produced, and to provide details about its connection to the radio jet, an analysis of simultaneous radio and  $\gamma$ -ray light curves is essential.

However, we highlight two caveats about the interpretation of radio/gamma correlation analyses, which have often been interpreted too simplistically. First, it is well-known that there is usually a considerable delay between mm and cm radio flares. Thus, although cm-flares would tend to peak after the  $\gamma$ -ray flares, mm-flares would show shorter delays or possibly even peak before the  $\gamma$ -rays. The very important second caveat is that a correlation analysis tends to measure the distance between the peaks, especially if the flares have different timescales (as the radio and the  $\gamma$ -ray flares tend to have ). However, a radio flare starts to grow a considerable time before it peaks. The *beginning* of a millimeter flare coincides with the ejection of a new VLBI component from the radio core [3]. This is the epoch that must be compared with the  $\gamma$ -ray flaring, not the epoch of the radio flare maximum. The crucial question is whether a  $\gamma$ -ray flare

occurs *before* the beginning of a mm-flare, or *after* it; in the former case the  $\gamma$ -rays originate upstream of the radio core (the beginning of the radio jet), in the latter, they originate downstream of the radio core, presumably from the same disturbances that produce the radio outbursts.

In this proceeding we summarize our recent results [4], obtained after combining the finely sampled 37 GHz Metsähovi light curves and the monthly binned  $\gamma$ -ray light curves provided by the *Fermi*/LAT First Source Catalog [1FGL, 5]. By using a radio flare decomposition method, we estimate the beginning epochs of millimeter flares and their phases during  $\gamma$ -ray flaring events to establish the true temporal sequence between  $\gamma$ -ray and radio flaring.

## II. THE 37 GHz AND $\gamma$ -RAY LIGHT CURVES

The Metsähovi quasar monitoring program currently includes about 250 AGN at 37 GHz. From them, we selected a sample of sources that fulfill the following criteria: (i) well-sampled light curves during the period 2007-2010, covering the 1FGL period, (ii) a firm association with the 1FGL catalogue, and (iii) a  $\gamma$ -ray monthly light curve during the 1FGL period that is significantly different from a flat one.

Our final sample consists of 60 sources classified according to their optical spectral type as highly polarized quasars (HPQ, 22), low polarization quasars (LPQ, 5), quasars without any optical polarization data (QSO, 15), BL Lac type objects (BLO, 17), and radio galaxies (GAL, 1). The sample of sources used

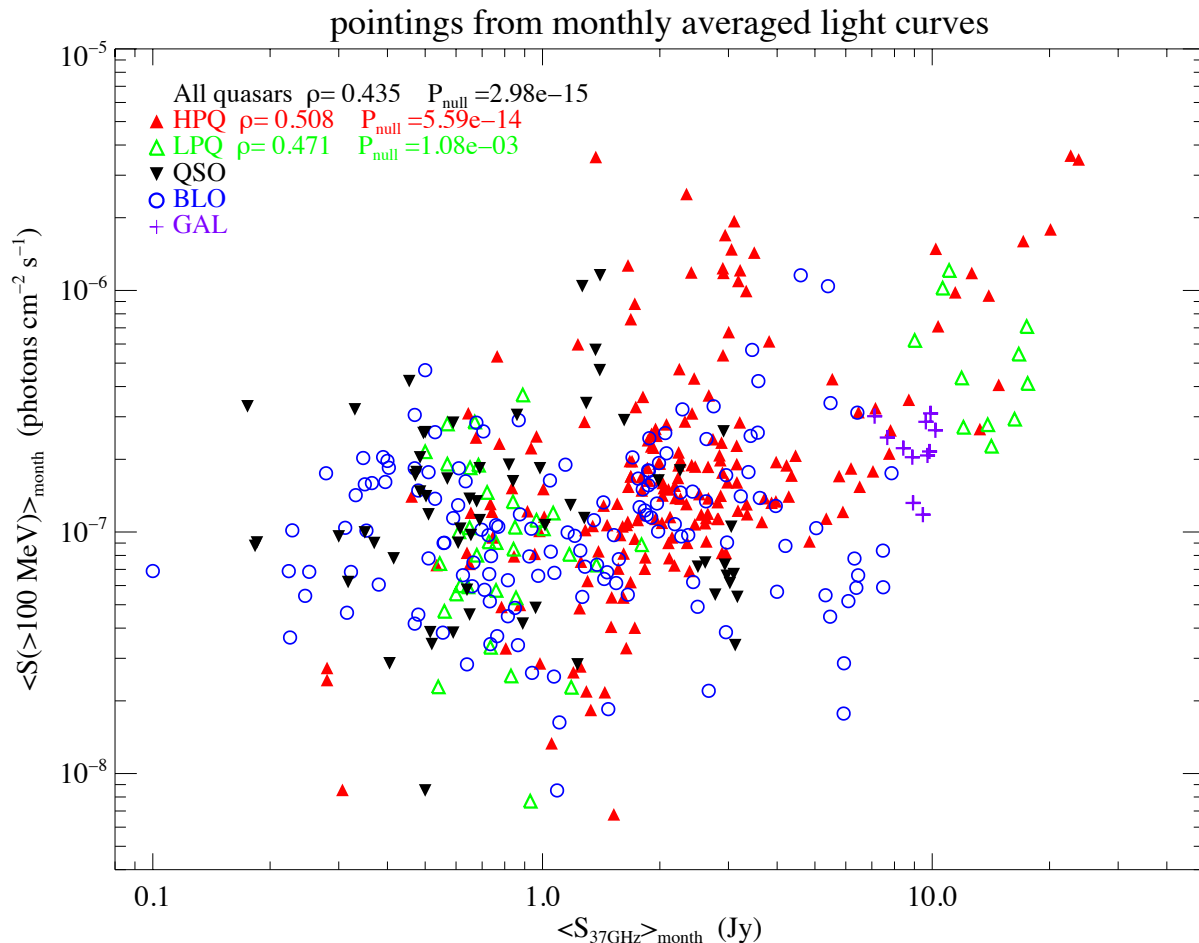


FIG. 1: Monthly flux-flux relation for the combined sample of 60 northern AGN. The different types of sources are symbol coded as shown in the legend, the correlations coefficients are shown only when the significance is  $> 99.9\%$ .

in this work is listed in Table 1 of [4]

### III. THE $S_{37\text{GHz}} - S_{\gamma}$ CORRELATION

To compare radio flux densities and  $\gamma$ -ray photon fluxes, monthly binned radio light curves were created from the Metsähovi light curves. The time bins are the same as in the 1FGL flux history curves, allowing us to compare simultaneously  $\gamma$ -ray photon flux and radio flux-density variations with the time resolution of a month.

Figure 1 shows that simultaneous measurements at the two bands appear to be positively correlated. However, we find significant differences between quasars and BL Lacs, which we describe below. By applying the Spearman's rank correlation test, two very clear results emerge. First, there is a significant positive correlation between the  $\gamma$ -ray photon flux and the 37 GHz flux density for quasars, while the BL Lac fluxes are not correlated. Second, the strength and

the significance of the correlations is different for each type of quasar.

The photon flux - flux density correlation for quasars is absent for QSOs, significant for LPQs, and very significant for HPQs. Such a dependence on the degree of optical polarization may arise naturally if the polarization indicates the viewing angle of the jet, with sources with high optical polarization having their jets oriented closest to our line of sight (see Figure 7 in [6]). The dependence of the flux - flux relation on optical polarization agrees with previous results, where it has been shown that the brightest  $\gamma$ -ray emitters have preferentially smaller viewing angles and consequently higher Doppler boosting factors [e.g., 2]. Since  $\gamma$ -ray fluxes and radio flux densities are significantly correlated for sources where the relativistic jet is aligned close to our line of sight, this implies that there is a strong coupling between the radio and the  $\gamma$ -ray emission mechanisms. That the correlation is seen on monthly timescales further indicates a cospatial origin in quasar-type blazars.

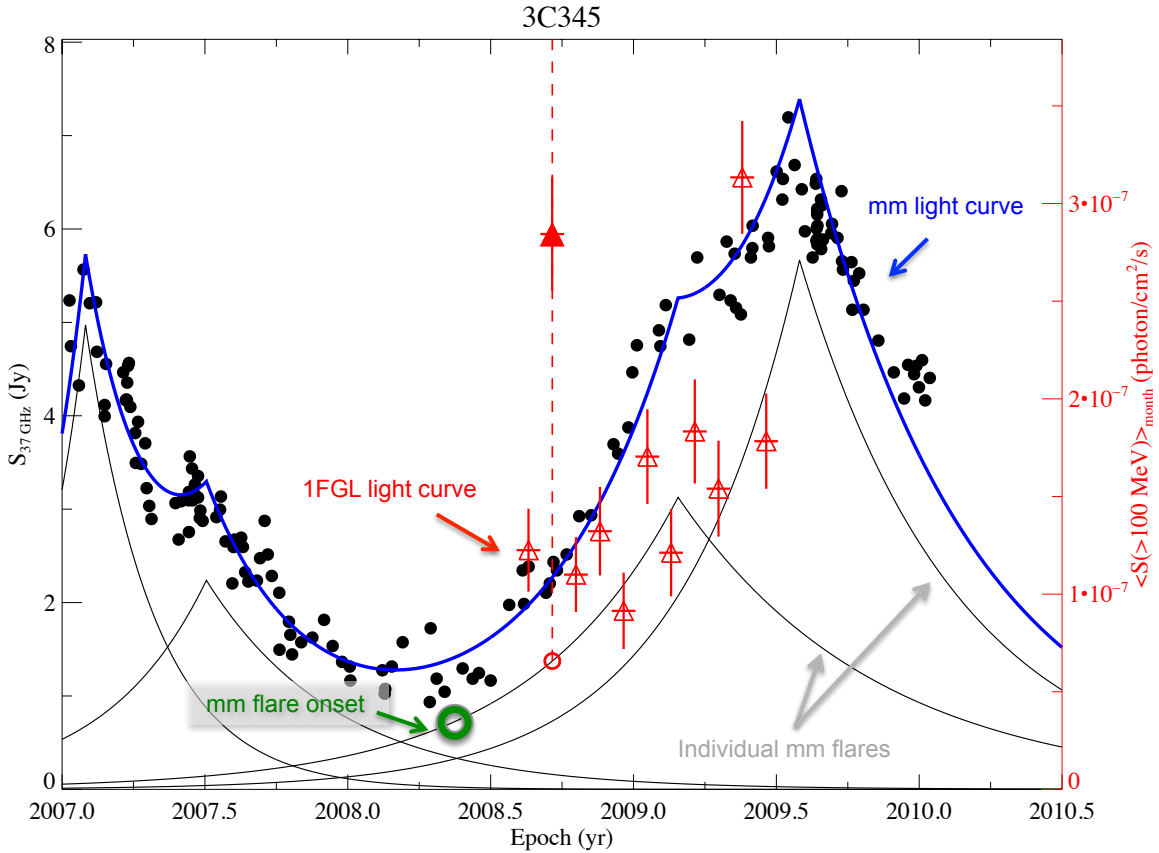


FIG. 2: The recent flux history at 37 GHz (filled circles) and  $\gamma$ -rays (triangles) of 3C 345. The total flux density has been decomposed using individual exponential flares. The filled triangle represents the most significant peak in the  $\gamma$ -ray flux density during the 1FGL period. The dashed vertical line is drawn to highlight the relation between the peak in the  $\gamma$ -ray light curve and the ongoing millimeter flare.

#### IV. CONNECTIONS BETWEEN ONGOING FLARES AND HIGH STATES OF GAMMA-RAY EMISSION

We have decomposed the mm light curves into individual exponential flares (see Figure 2), each of which corresponds to a new disturbance created in the jet and is often detectable as a new VLBI component [3]. We further calculate the phase of the mm-flare when the most prominent maxima in the 1FGL light curves occurred. Our analysis shows that the most significant  $\gamma$ -ray flux peaks tend to occur when a mm-flare is either rising or peaking. This indicates that the strong  $\gamma$ -ray flares are produced in the same disturbances that produce the mm flares.

Using our data, we can estimate the time delay between the time when the mm flare starts and when the  $\gamma$ -rays peak for each source. We define the beginning

of a mm flare to be:

$$t_0^{mm} = t_{max}^{mm} - \tau, \quad (1)$$

where  $t_{max}^{mm}$  is the time of the mm flare peak and  $\tau$  is the variability timescale. In other words, we define the beginning of the flare as the epoch when its flux is  $1/e$  of the maximum flux,  $S(t_0^{mm}) = \frac{S_{max}^{mm}}{e}$ . For each source we estimate the time delay between the time of mm-flare onset (green circle in Figure 2) and when the  $\gamma$ -ray peak occurs (filled triangle in Figure 2). The observed time delay has a distribution centered around 70 days with the onset of the mm-flare preceding the  $\gamma$ -ray peak.

After converting the time delays to linear distances from the region where the mm-outburst begins (i.e. the radio-core) to the region of the  $\gamma$ -ray production, our estimates lead us to conclude that in our sample the average location of the  $\gamma$ -ray emission region is about 7 parsecs downstream the radio-core.

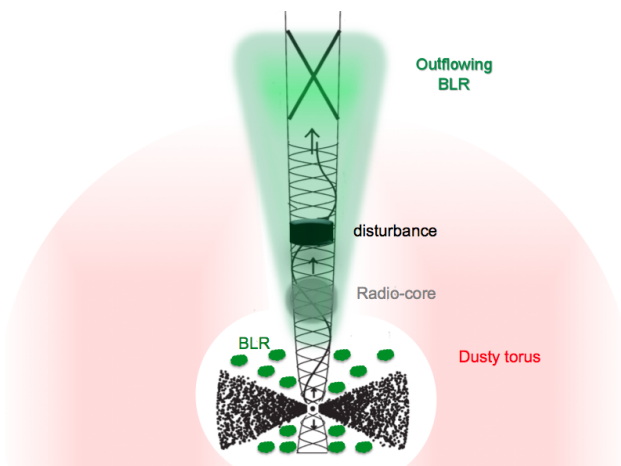


FIG. 3: Sketch of the inner parts of an AGN. Recent results [13, 14] have shown that a significant amount of broad-line emission is driven by optical continuum radiation produced downstream of the radio core, this strongly suggests the presence of an additional component of the BLR located at parsec scales. In this scenario, an outflowing BLR may serve as a source of seed-photons to produce  $\gamma$ -rays via EC models far away from the central engine [4].

## V. SUMMARY AND DISCUSSION

The results presented in [4] strongly indicate that at least for the strongest  $\gamma$ -rays the production sites are downstream or within the radio core [7], well outside the BLR at distances of several parsecs or even tens of parsecs from the black hole and the accretion disk. A number of papers based on *Fermi* data have reached similar conclusions [e.g. 8].

In the current AGN paradigm, it is widely believed that  $\gamma$ -ray are produced via Inverse Compton (IC) mechanisms in the relativistic jet, and the seed photons for the IC process may be provided by the jet synchrotron emission (Synchrotron Self Compton, SSC) as well as by external photon sources (External Compton, EC) such as an accretion disk, the broad-line re-

gion (BLR) or the hot dusty torus. At the distance of 7 parsecs from the radio core – keeping in mind that the radio core itself is often at a considerable distance from the black hole [e.g. 9] – the only sources of seed photons for the IC processes are the jet itself and the dusty torus. However, there is growing evidence [13, 14] that the BLR might extend to much larger distances than given by virial estimates ( $R_{BLR} < 1 pc$ ). One possibility is that the jet drags a part of the BLR with it, see Figure 3 for a sketch of an outflowing BLR among the other inner AGN constituents.

While single zone SSC has failed to reproduce the observed  $\gamma$ -rays [10] and so far there are only a couple of blazars with firm detections of a dusty torus [11, 12], a tentative idea to test is *whether an outflowing BLR can serve as a source of external photons to produce  $\gamma$ -rays, even at distances of parsecs downstream of the radio-core*. In this scenario, the strong  $\gamma$ -ray events are produced in the same disturbance that produces the radio outburst by upscattering external photons provided by an outflowing BLR.

The most effective way to explore any of the above scenarios (and others) is by modeling simultaneous, well-sampled spectral energy distributions (SEDs) [15, 16] following a multizone modeling approach [17]. Furthermore, recent results have suggested that the more massive the black hole is, the faster and the more luminous jet it produces [18]. Therefore, a reliable estimate of the black hole masses is an essential input to theoretical models of both the shape and the variability of blazars SEDs.

## Acknowledgments

We acknowledge the support from the Academy of Finland to our AGN monitoring project (project numbers 212656, 210338, 122352 and others).

- 
- [1] Ackermann, M., Ajello, M., Allafort, A., et al., arXiv:1108.0501 (2011)
  - [2] Lister, M. L., Aller, M., Aller, H., et al., arXiv:1107.4977 (2011)
  - [3] Savolainen, T., Wiik, K., Valtaoja, E., Jorstad, S. G., & Marscher, A. P., *A&A*, 394, 851 (2002)
  - [4] León-Tavares, J., Valtaoja, E., Tornikoski, M. et al., *A&A*, 532, A146 (2011)
  - [5] Abdo, A. A., Ackermann, M., Ajello, M., et al., *ApJS*, 188, 405 (2010)
  - [6] Niippola, E., Valtaoja, E., Tornikoski, M. et al., arXiv:1109.5844 (2011)
  - [7] Pushkarev, A. B., Kovalev, Y. Y., & Lister, M. L., *ApJL*, 722, L7 (2010)
  - [8] Agudo, I., Jorstad, S. G., Marscher, A. P., et al., *ApJL*, 726, L13 (2011)
  - [9] Marscher, A. P., Jorstad, S. G., D’Arcangelo, F. D., et al., *Nature*, 452, 966 (2008)
  - [10] Lindfors, E. J., Valtaoja, E., Türler, M., *A&A*, 440, 845 (2005)
  - [11] Türler, M., Chernyakova, M., Courvoisier, T. J.-L., et al., *A&A*, 451, L1 (2006)
  - [12] Malmrose, M. P., Marscher, A. P., Jorstad, S. G., Nikutta, R., & Elitzur, M., *ApJ*, 732, 116 (2011)
  - [13] Arshakian, T. G., León-Tavares, J., Lobanov, A. P., et al., *MNRAS*, 401, 1231 (2010)
  - [14] León-Tavares, J., Lobanov, A. P., Chavushyan, V. H., et al., *ApJ*, 715, 355 (2010)

- [15] Planck Collaboration, Aatrokoski, J., Ade, P. A. R., et al., arXiv:1101.2047, (2011)
- [16] Giommi, P., Polenta, G., Lahteenmaki, A., et al., arXiv:1108.1114, (2011)
- [17] Türler, M., & Björnsson, C.-I., arXiv:1109.2518, (2011)
- [18] León-Tavares, J., Valtaoja, E., Chavushyan, V. H., et al., *MNRAS*, 411, 1127 (2011)